Geophysical Research Letters

RESEARCH LETTER
10.1029/2020GL088986

Model Forecast Error Correction Based on the Local Dynamical Analog Method: An Example Application to the ENSO Forecast by an Intermediate Coupled Model

Zhaolu Hou[1], Bin Zuo[1], Shaoqing Zhang[1,2,3], Fei Huang[1], Ruiqiang Ding[4], Wansuo Duan[5], and Jianping Li[1,2]

[1]Frontiers Science Center for Deep Ocean Multispheres and Earth System (FDOMES)/Key Laboratory of Physical Oceanography/Institute for Advanced Ocean Studies, Ocean University of China, Qingdao, China, [2]Laboratory for Ocean Dynamics and Climate, Pilot Qingdao National Laboratory for Marine Science and Technology (QNLM), Qingdao, China, [3]International Laboratory for High-Resolution Earth System Model and Prediction (iHESP), College Station, TX, USA, [4]State Key Laboratory of Earth Surface Processes and Resource Ecology, Beijing Normal University, Beijing, China, [5]State Key Laboratory of Numerical Modeling for Atmospheric Sciences and Geophysical Fluid Dynamics, Institute of Atmospheric Physics, Chinese Academy of Sciences, Beijing, China

Key Points:
- Analogs based on historical forecast can be used to estimate model forecast error and correct model forecasts
- The Local Dynamical Analog method can locate high quality analogs based on the initial and evolutional information
- Analog correction using the Local Dynamical Analog improves ENSO forecast skill, significantly in root-mean-squared error skill

Supporting Information:
- Supporting Information S1

Correspondence to:
J. Li,
ljp@ouc.edu.cn

Citation:
Hou, Z., Zuo, B., Zhang, S., Huang, F., Ding, R., Duan, W., & Li, J. (2020). Model forecast error correction based on the local dynamical analog method: An example application to the ENSO forecast by an intermediate coupled model. *Geophysical Research Letters*, *47*, e2020GL088986. https://doi.org/10.1029/2020GL088986

Received 27 MAY 2020
Accepted 6 SEP 2020
Accepted article online 14 SEP 2020

Abstract Numerical forecasts always have associated errors. Analog correction methods combine numerical simulations with statistical analyses to reduce model forecast errors. However, identifying appropriate analogs remains a challenging task. Here, we use the Local Dynamical Analog (LDA) method to locate analogs and correct model forecast errors. As an example, an El Niño–Southern Oscillation (ENSO) intermediate coupled model forecast error correction experiment confirms that the LDA method locates high quality analogs of states of interest and improves the model forecast performance, which is due to the initial and evolution information included in the LDA method. In addition, the LDA method can be applied using a scalar time series, which reduces the complexity of the dynamical system. The LDA method is a promising method to locate dynamic analogs and can be applied to existing numerical models and forecast results.

Plain Language Summary Earth-science models are important tools in the analysis of physical processes and in forecasts of future conditions. However, numerical models always contain forecast errors. Model forecast error in historical data may appear again. Thus, the historical model forecast error can be used to correct the forecast results of focused states, which can reduce the model forecast error without building the new numerical model. The key question is how to locate suitable historical model forecast errors for the focused states. In this paper, we use the Local Dynamical Analog (LDA) method to locate the model forecast error and firstly correct the model forecast results. In the ENSO prediction experiment by an intermediate coupled model, the LDA is proved the advantage over other analog-locate methods to find analogs and improve the whole forecast skill and the ENSO event forecast. The improvement from the LDA method in the root squared mean error skill is significant, and the forecast intensity of ENSO events is closer to observation than that of the uncorrected forecast.

1. Introduction

Earth-science models are important tools in the analysis of physical processes and in forecasts of future conditions. For example, the El Niño–Southern Oscillation (ENSO) system, an important atmosphere–ocean coupling process, is routinely simulated by many dynamical and statistical models for forecast and research purposes (e.g., McPhaden et al., 2006; Tang et al., 2018). Despite improvements in modeling capabilities and the growing availability of computational resources, model forecasts remain limited by model errors. In recent decades, extensive efforts have been made to reduce model errors by improving physical parameterizations, and model prediction initialization by developing advanced data assimilation techniques (e.g., Duan et al., 2014; Zhang, 2011a, 2011b; Zhang et al., 2007, 2012; Zhu et al., 2012; Zhu, Kumar, Lee, 2017; Zhu, Kumar, Wang, 2017). However, model forecast errors cannot be entirely eliminated using these strategies alone. Model forecast error correction can be used to further improve forecast accuracy. Methods to correct

model forecast errors can be divided into state-independent and state-dependent groups (Danforth & Kalnay, 2008). State-independent corrections can reduce systematic error, and are frequently used, which include methods such as model output statistics (MOS) (Carter et al., 1989; Glahn & Lowry, 1972). However, system error accounts for about 20% of the total model forecast error, while non-systematic error accounts for about 80% of the total error (Dalcher & Kalnay, 1987). Other results have indicated that State-independent or "systematic error" correction, which does not depend on state and is held constant throughout the integration, does not improve the forecast skill of the model (DelSole et al., 2008; Delsole & Hou, 1999). Therefore, state-dependent corrections are needed to reduce the remaining nonsystematic error components.

Earth science has benefited from the proliferation of satellite data, in situ monitoring, and numerical simulations in recent decades. The availability of such data sets facilitates the identification of states analogous to a dynamic system of interest (Lorenz, 1969). Analogs have been demonstrated to be applicable in inversions and estimations of the evolving trajectories of a dynamic system (Hamill & Whitaker, 2006; Lguensat et al., 2017). Ren et al. (2006) showed that state-dependent model forecast errors of analogous model states selected according to their initial states are to some degree similar to those of the states of interest and proposed a corresponding analog correction method. An important feature of analog correction methods is that they do not require new models to be built and can be applied to existing numerical models and forecast results (Liu & Ren, 2017; Ren et al., 2006; Ren & Chou, 2007). A key challenge in the application of analog correction methods is how to identify analogous model states. One method currently used to select analog states is based on the spatial correlation coefficient between present and historical initial field anomalies (Bergen & Harnack, 1982; Liu & Ren, 2017; Van den Dool, 1987). However, this method is based solely on the similarity of the initial states and does not consider similarities in evolution. In addition, the spatial region used to calculate the correlation has a large effect on the analog quality. Thus, more effective analog selection schemes based on dynamics are needed.

In the field of predictability research, the nonlinear local Lyapunov theory also involves using analogs to estimate system predictability (e.g., Li et al., 2018; Li & Ding, 2011, 2013, 2015). Li and Ding (2011) proposed the Local Dynamical Analog (LDA) method and demonstrated the benefits of this approach in locating analogous states in comparison with other analog location methods. The LDA method ensures similarity between the dynamical evolution of both states in addition to requiring similarity in their initial states. Therefore, the LDA method is more effective in finding analogous trajectories than are other techniques and can improve analog-based model error corrections.

Thus, we apply the LDA method to model forecast error corrections using analogs and explore the benefits of the LDA method compared with other analog selection schemes. The methods and model used in this study are introduced in the next section. The performance of selected analogs is presented in section 3, and the model forecast correction procedure and results are described in section 4. Section 5 presents the main conclusions and a related discussion.

2. Methodology and Model

2.1. Method

Model forecasts are typically based on the following discrete state equation:

$$\mathbf{y}_{f,j}(t_i) = \mathbf{M}_{i \to (i+j)}(\mathbf{y}_a(t_i)), \tag{1}$$

where $\mathbf{M}_{i \to (i+j)}$ is the dynamical forecast from initial time t_i to final time t_{i+j}; $\mathbf{y}$ is the system state; a multidimensional vector, $\mathbf{y}_a(t_i)$, represents the observational state of the dynamical system at time t_i, which is used as the forecast initial state; $j \cdot \Delta$ is the forecast lead time (Δ represents model output interval time and j is the model output step); and $\mathbf{y}_{f,j}(t_i)$ is the forecast state at time t_{i+j}. However, because of model deficiency, the forecast state $\mathbf{y}_{f,j}(t_i)$ includes some error compared with its observation $\mathbf{y}_a(t_{i+j})$. The model forecast error from the initial time t_i to time t_{i+j} can be described as follows:

$$e_j(t_i) = \mathbf{y}_{f,j}(t_i) - \mathbf{y}_a(t_{i+j}). \tag{2}$$

Analog-based correction methods for model forecast errors make use of forecast errors from analogs in historical data. For the state $\mathbf{y}_a(t_i)$, its analog state $\mathbf{y}_a(t_k)$ has the forecast state $\mathbf{y}_{f,j}(t_k)$, and its corresponding

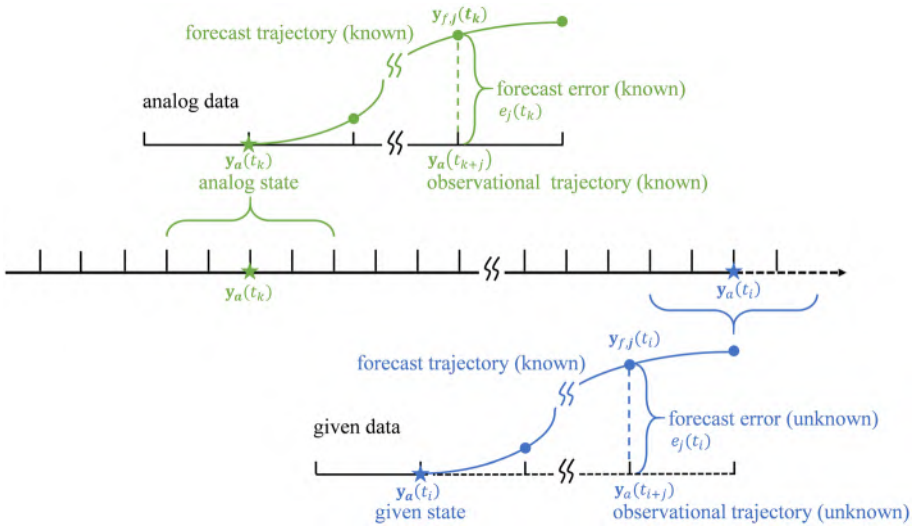

Figure 1. Schematic representation of model forecast correction using analogous data. The black lines represent observational data. $\mathbf{y}_a(t_i)$ is the focused observational state at the time t_i and $\mathbf{y}_a(t_k)$ represents its analog in historical observational data. The blue curve is the forecast results from $\mathbf{y}_a(t_i)$ and the green curve is that from $\mathbf{y}_a(t_k)$. $\mathbf{y}_{f,j}(t_i)$ is the forecast at the lead time of j from the initial state $\mathbf{y}_a(t_i)$, which is the forecast of $\mathbf{y}_a(t_{i+j})$. $\mathbf{y}_{f,j}(t_k)$ corresponds to that from the initial state $\mathbf{y}_a(t_k)$, which is the forecast of $\mathbf{y}_a(t_{k+j})$. $e_j(t_k)$ is the difference between $\mathbf{y}_a(t_{k+j})$ and $\mathbf{y}_{f,j}(t_k)$. $e_j(t_i)$ is that between $\mathbf{y}_a(t_{i+j})$ and $\mathbf{y}_{f,j}(t_i)$. When forecasting the future states from $\mathbf{y}_a(t_i)$ at the time t_i, we can obtain the forecast error $e_j(t_k)$ of its analog state in advance and correct the forecast $\mathbf{y}_{f,j}(t_i)$ with $e_j(t_k)$.

model forecast error $e_j(t_k)$ can be obtained (as shown in Figure 1). Thus, the focused forecast state $\mathbf{y}_{f,j}(t_i)$ at time t_{i+j} can be corrected by the known error $e_j(t_k)$. The corrected forecast can be calculated as

$$\widehat{\mathbf{y}}_{f,j}(t_i) = \mathbf{y}_{f,j}(t_i) - \left[\mathrm{a} \cdot e_j(t_k) + \mathrm{b}\right], \tag{3}$$

where a, b is the undetermined parameters, which can be obtained by the linear regression method based on the historical training data. In an operational environment, the model forecast results of multiple analogous states can be used to offset the uncertainty of a single forecast state.

The general approach of the LDA method is to find local analogs of a pattern of state evolution in an observational time series. For state $\mathbf{y}_a(t_i)$ and its analog $\mathbf{y}_a(t_k)$ in the historical data, the initial distance d_i between the two states is given by $d_i = |\mathbf{y}_a(t_i) - \mathbf{y}_a(t_k)|$. Within the evolutionary interval L, the evolutionary distance d_e is given by $d_e = \sqrt{\frac{1}{L}\sum_{l=1}^{L}|\mathbf{y}_a(t_{i-l}) - \mathbf{y}_a(t_{k-l})|^2}$. The total distance d_t, considering both the initial distance and the evolutionary distance, is found by adding d_i and d_e. If d_t is very small, it is highly likely that the states $\mathbf{y}_a(t_i)$ and $\mathbf{y}_a(t_k)$ are analogous. Thus, the LDA method locates analogs using information from both the initial state and its evolution. In contrast, traditional approaches to locating analogous states only consider similarities in initial spatial structures, ignoring dynamic information. Although the equations of the LDA method are expressed by the multidimensional field variable $\mathbf{y}_a(t_i)$, the LDA method can also be applied to scalar time series.

2.2. Model and Data

To evaluate the LDA method, we correct the forecast results of the Zebiak–Cane (ZC) model from January 1856 to December 2018, specifically the Niño 3.4 index time series. The initial field for the model uses sea-surface temperature anomalies (SSTa) from the Kaplan data set (Kaplan et al., 1998), and the forecast lead time is 0–12 months. The ZC model has been widely used in predictions and predictability studies of ENSO (e.g., Chen et al., 2004; Duan & Zhao, 2015; Hou et al., 2018; Mu et al., 2007). The development of the ZC model is ongoing, with continual improvements to ENSO predictions. Chen et al. (2004) carried out the first retrospective forecast experiment spanning the past 150 years, using only reconstructed SST data for model initialization. Note that the MOS scheme is already used to correct state-independent forecast

errors in this model. Here, we use the same configuration as Chen et al. (2004) to forecast SST and apply the state-dependent correction from 1856 to 2018.

3. Identifying Analogous States

The first step in forecast error analog correction is to locate analogs. Here, we describe how we identify analogous states for the ZC model and assess its performance.

3.1. Configuration of Analog Location Methods

The LDA method is used to locate analogs based on scalar time series observational data sets of the Niño 3.4 index (average SSTa over the region 5°N–5°S, 170°W–120°W) from January 1856 to December 2018, which corresponds to a total of 1956 states. In the ZC model, Δ is 1 month and the evolutional interval L is set to 3 months due to the autocorrelation coefficient (greater than 0.8) (Li & Ding, 2011). The temporal distance between a state and its analogs must exceed 24 months to avoid similarities caused by the persistence of data. The analogs must also be from the same season as the state of interest. Forecast error of a single analog includes certain random parts. Thus, the average of forecast errors from the five best analogs located by the LDA method is applied to correct the forecast of the focused state, to reduce instability of the correcting performance.

For comparison, the field correlation method (Liu & Ren, 2017) is also used to locate analogs. For two vector states $\mathbf{y}_a(t_i)$ and $\mathbf{y}_a(t_k)$, the spatial correlation coefficient r, which can describe the similarity between them, is written as $\frac{\langle \mathbf{y}_a(t_i), \mathbf{y}_a(t_k) \rangle}{|\mathbf{y}_a(t_i)||\mathbf{y}_a(t_k)|}$, where $\langle , \rangle$ represent a vector inner product, $||$ is vector norm. In the ZC model, $\mathbf{y}_a(t_i)$ is the SSTa field over the Niño 3.4 region of the observational data. The maximum correlation between $\mathbf{y}_a(t_i)$ and $\mathbf{y}_a(t_k)$ is used to select analogs. This scheme is referred to as the SST field analog (SFA). Other elements of the SFA method are consistent with those of the LDA method.

In order to highlight the importance of evolutionary information, the analogs are located just by the initial distance d_i, which is refined as the local analog (LA) method. Other elements of the LA method are consistent with those of the LDA method.

3.2. Analog Performance

Here, we evaluate the performance of the analogs selected using the LDA, LA, SFA methods. Because two states that are close to each other in phase space should, to some degree, evolve in a similar fashion, we focus our analysis on whether the observed states retain similar features over time. We also check whether this similar feature in the observation data can be reflected on the model forecast states and model forecast error.

For each state $y_a(t_i)$ and its analog $y_a(t_k)$, we consider a 12-month Niño 3.4 index sequential observational time series from the initial time as the observational trajectory $(y_a(t_{i+j}), j = 0,1,2,...,12)$ and $(y_a(t_{k+j}), j = 0,1,2,...,12)$.The similarity of the focused state and its analog can be determined using the correlation coefficient and the root-mean-squared error (RMSE) of the whole period (from January 1856 to December 2018) for different lead times. The correlation coefficient and RMSE can be calculated as follows:

$$\mathrm{Corr(obs)}_j = \frac{\mathrm{Cov}\left(y_a\left(t_{i+j}\right), y_a\left(t_{k+j}\right)\right)}{\mathrm{Var}(y_a(t))} = \frac{\sum_{i=1}^{N}\left(y_a\left(t_{i+j}\right) - \bar{y}_a\right) \cdot \left(y_a\left(t_{k+j}\right) - \bar{y}_a\right)}{\sum_{i=1}^{N}\left(y_a(t_i) - \bar{y}_a\right)^2}, \tag{4}$$

$$\mathrm{RMSE}_j = \sqrt{\frac{\sum_{i=1}^{N}\left(y_a\left(t_{i+j}\right) - y_a\left(t_{k+j}\right)\right)^2}{N}}, \tag{5}$$

where i represents the focused state and k is its analog, N is the total number of the states considered, equal to 1956 from January 1856 to December 2018, $j = 0,1,2,...,12$, is the lead time (month). Noting, the state $y_a(t_k)$ is the average results of the five best analogs for the state $y_a(t_i)$.

The correlation and RMSE for the evolution of observational data are shown in Figures 2a and 2b. The correlations from different methods are all positive, although decreasing with lead time (Figure 2a). This suggests that similar features between the state of interest and its analogs are maintained during the subsequent evolution. Noting, the correlation from the LDA method is about 0.2 larger than that of the

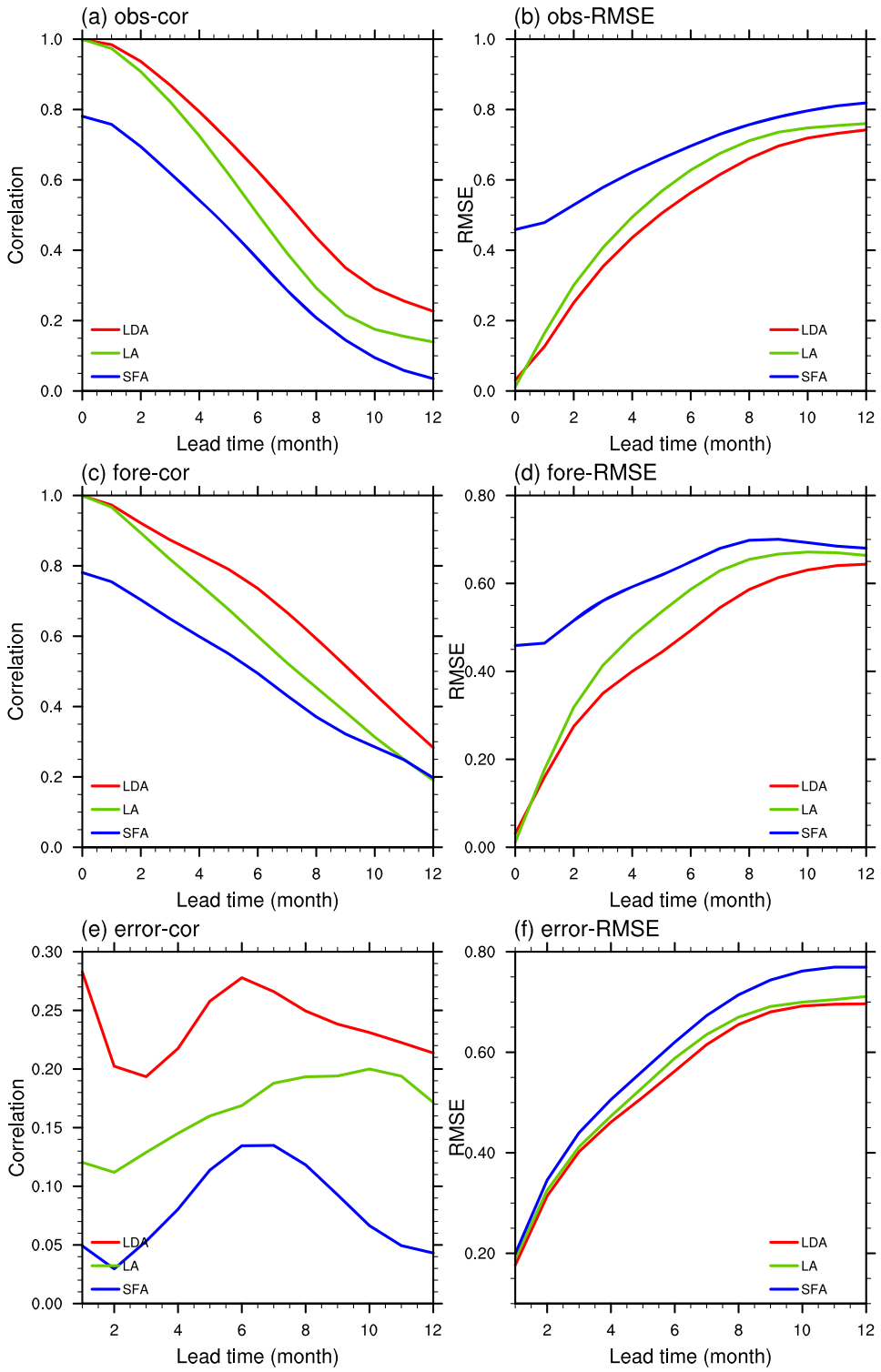

Figure 2. The performance of analog from different method: (a) Correlation coefficient and (b) RMSE between observational Niño 3.4 states and their analogs from the LDA (red line), SFA (blue line), and LA (green line) methods. (c, d) as the same with (a, b) but for model forecasts. (e, f) as the same with (a, b) but for model forecast errors.

SFA method and the differences using statistical bootstrapping differences are significant at the $\alpha = 0.1$ level. The RMSE of the LDA and SFA methods increases with lead time (Figure 2b) and that of the LDA method is smaller than the SFA method for all lead times. The LA method is also better than the SFA method in both correlation and RMSE (Figures 2a and 2b; green line). This can be attributed to the low dimensionality of the Niño 3.4 index time series used to locate analogs with the LDA/LA method. In contrast, the Niño 3.4 area field used by the SFA method is of higher dimension, meanwhile high correlation between SSTa over Niño 3.4 region may have worse performance of Niño 3.4 index time series due to the feature of correlation formula. The performances of the LDA and LA methods also are different. At a 0-month lead time, the analog from the LA method outperforms that from the LDA method in terms of RMSE. This is because the LA method puts more importance on similarities in the initial state. However, with increasing lead time, the RMSE from the LDA method falls below that of the LA method and the correlation from the LDA method becomes larger, which highlights the importance of evolutionary information in locating analogs. Figures 2c and 2d show the correlation and RMSE between model forecast results for an initial state and its analogs at different lead times, which also indicates that analogs selected from observational data maintain their similarity for model forecast results. The comparison of the LDA and LA methods further shows the important role of evolutionary information in locating analogs. In summary, the LDA method has better performance than does the SFA method, which is due to the high-quality analogs located by the LDA method.

The analog performance between the forecast error of the state and its analogs at different lead times is shown (Figures 2e and 2f). The correlations from the LDA method are ~0.2 greater than those of the SFA method for all lead times and using statistical bootstrapping differences are significant at the $\alpha = 0.1$ level. Due to random fraction in forecast error, correlation does not always consistently decrease as lead time increasing. The noticeable variation of the LDA correlation with lead time is caused by the fact that model forecast errors are affected by many factors. Comparing to the LA and SFA methods, we find that the LDA method has better performance in correlation and RMSE skill, which is consistent with the results from the observation trajectories (Figures 2a and 2b) and model forecast trajectories (Figures 2c and 2d). This indicates that the higher-dimensional SFA method finds fewer high-quality analogs than does the LDA, which operates on a lower-dimensional system, with the same amount of data. We also check the influence of the parameters of the LDA method on the analog performance, and the results show that the LDA method always have some advantages over other methods (shown in the supporting information).

In summary, the analog location methods investigated here can retrieve analogs of model forecast errors from observations. The performance of the LDA method is better than that of the SFA and LA method in both correlation and RMSE skill. Unlike the LA method, the LDA method considers evolution information of the dynamical system and has the best similarity in the forecast error trajectories. Thus, historical analog forecast errors from the LDA method may have the capacity to improve model forecast skill.

4. Forecast Error Correction

After identifying the analogous states and their corresponding forecast errors, we next correct the forecast errors of states of interest. The analog-based error correction process is as follows: Firstly, for state $\mathbf{y}_a(t_i)$, locate its five best analogous states $\mathbf{y}_a(t_k)$ with the LDA method. Secondly, obtain the average of observation trajectories and forecast trajectories from the five best analogous states, then calculate the difference as the forecast error of the analogs $e_j(t_k)$. Thirdly, use $e_j(t_k)$ to correct the model forecast $\mathbf{y}_{f,j}(t_i)$ by linear regression. The linear regression parameters a, b are obtained by a least-square fitting between $e_j(t_{o_k})$ and $e_j(t_o)$ in historical training data.

The forecast skill for uncorrected and corrected Niño 3.4 index is verified by calculating correlation and RMSE between model forecasts and observations. Figure 3a shows the correlation skill for Niño 3.4 index during 1856–2018, where the shade area represents the confident level of 10% to 90% by bootstrapping (10,000 times resampling). The results for the LDA method are consistently higher than those of the raw forecasts, with the biggest improvements seen at the lead times of 6–12 months. Correlation coefficients averaged over 1–12 lead months are 0.729 for the LDA-corrected forecasts and 0.717 for the raw forecasts. The LDA-corrected forecast has higher correlation scores, but those scores are not statistically significant at the $\alpha = 0.1$ level based on bootstrapping. The RMSE scores are shown in Figure 3b. The RMSEs for the corrected forecasts from the LDA methods are smaller than the raw forecast: The average RMSE values

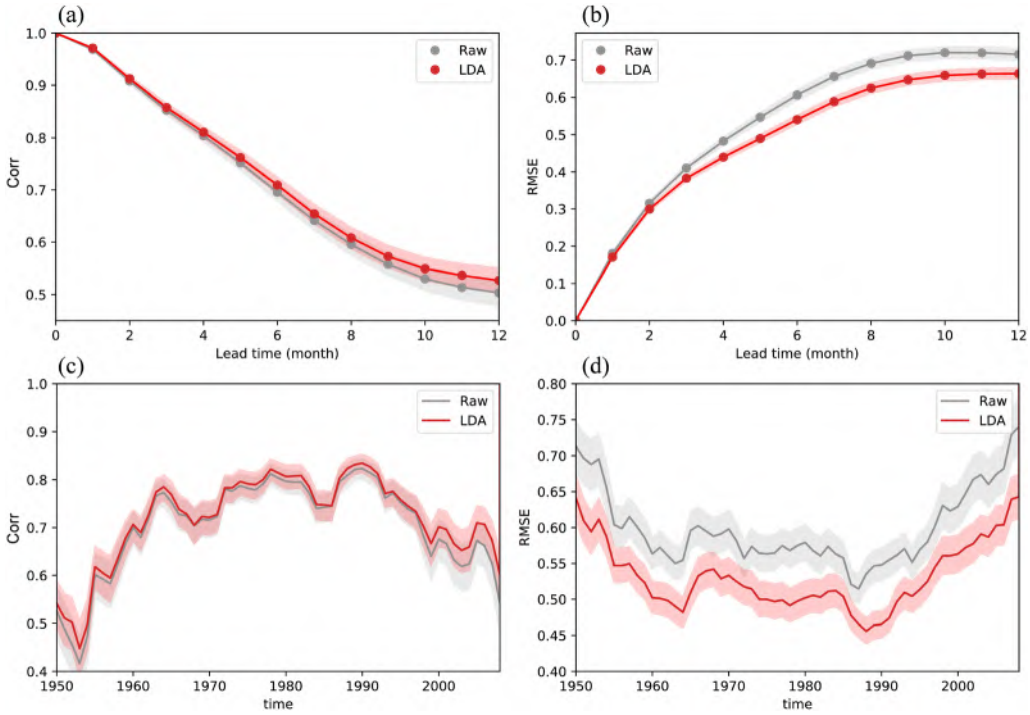

Figure 3. The skill performance of the raw and LDA-corrected model forecast: (a) Correlation coefficient skill and (b) RMSE skill for the raw model forecast (gray line), the LDA-corrected model forecast (red line) for January 1856 to December 2018; (c,d) are the forecast skill at the 6-month lead time since 1950 using a 21-year running window. Raw is the uncorrected model forecast results.

over 1–12 lead months are 0.519 for the raw forecasts, and 0.474 for the LDA method, whose difference passes the significant level of 0.1 with bootstrapping. The LDA method reduces the RMSE by 0.05°C for lead times of 10–12 months compared with the raw forecasts.

Because the ENSO forecast skill shows a clear interdecadal variation (e.g., Kirtman & Schopf, 1998; Tang et al., 2018), we assess the skill performance of the corrected forecast results using a 21-year running window. As SST data since 1950 are of higher quality, we focus on the period from January 1950 to December 2008. Figures 3c and 3d show the correlation and RMSE skill during different decadal periods at the lead time of 6 months, respectively. The LDA correction method can improve the performance of model forecasts during different decades, as is particularly evident in RMSE skills with the decrease by 0.05°C. The RMSE skill differences between the LDA-correcting and raw model forecast pass the significant level of 0.1 over nearly the whole periods. The correlation skill of the LDA-corrected forecast are always larger than that of the raw model forecast but are not statistically significant at the $\alpha = 0.1$ level based on bootstrapping. The forecast skill for the Niño 3.4 index has declined since the 1990s, most noticeably in the 21st century, as is reflected in the decreasing correlation coefficient (0.8 to 0.6) and the increasing RMSE (0.55 to 0.70).

The Niño 3.4 index provides information about ENSO events. ENSO events consist of cold and warm events that significantly impact the global climate (e.g., Wang et al., 2017). Thus, we evaluate the performance of the analog correction for ENSO event forecasts. We selected strong ENSO events which the intensity is over 1.5°C since 1950. El Niño events comprise of 1957/1958, 1965/1966, 1972/1973, 1982/1983, 1987/1988, 1991/1992, 1997/1998, 2015/2016. La Niña events include 1973/1974, 1975/1976, 1988/1989, 1998/1999, 1999/2000, 2007/2008, 2010/2010. The forecast results at the lead time of 6 months are shown in Figure 4. For the composited El Niño event, the raw forecast values are lower than observation in the developing phases and greater in the decaying phases. Through corrected by the LDA method, the forecast results are slightly improved in the developing phases. For the El Niño decaying phase, the higher forecast values also are reduced by the LDA method. Specially, the El Niño mature value from the corrected forecast is closer to observation. For the composited La Nina event, the correction from the LDA method also improves the

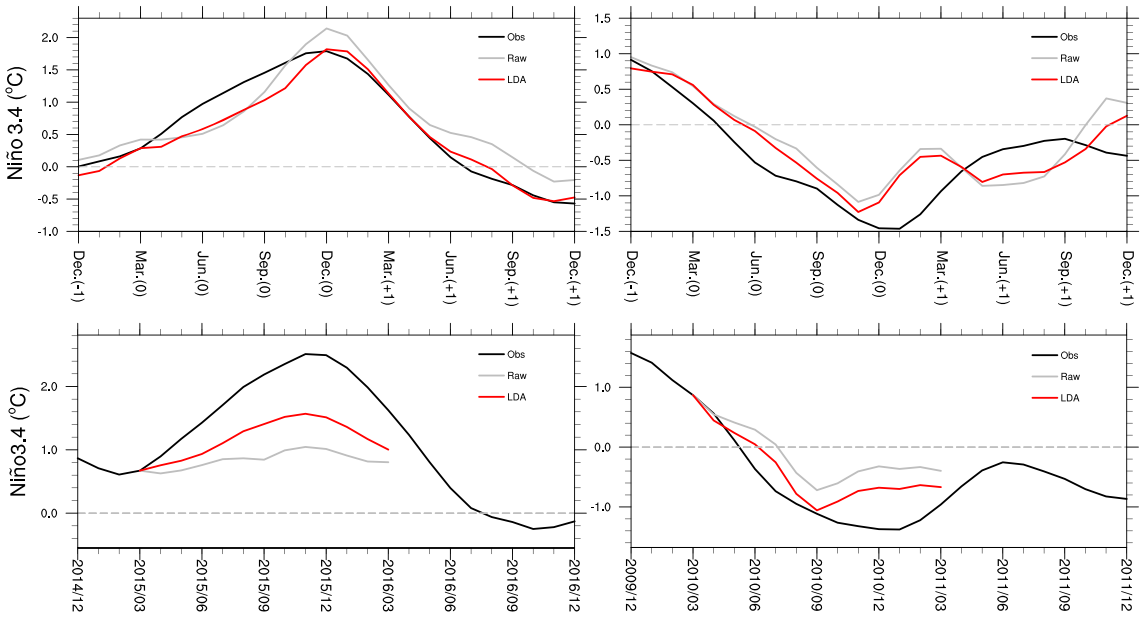

Figure 4. The ENSO event results of the raw and LDA-corrected model forecast: (a) is the composited strong El Niño event since 1950 (1957/1958, 1965/1966, 1972/1973, 1982/1983, 1987/1988, 1991/1992, 1997/1998, 2015/2016) and (b) corresponds to the composited strong La Nina event (1973/1974, 1975/1976, 1988/1989, 1998/1999, 1999/2000, 2007/2008, 2010/2010). (c) is the model forecast results of the 2015/2016 El Niño event and (d) is that of the 2009/2010 La Niña event, beginning in March 2015 and March 2010, respectively. Raw is the uncorrected model forecast results.

forecast performance of the ZC model. These results show that the LDA method can improve the ENSO event forecast performance.

In additional, we choose two recent strong events, El Niño event (2015/2016) and La Niña event (2010/2011), to assess forecast results from the raw forecast and LDA-corrected forecasts (Figures 4c and 4d). As ENSO forecast suffers from a spring predictability barrier (e.g., Jin et al., 2008), we focus on forecast results starting in March. For 2015/2016, the raw forecast shows a weak El Niño occurring in winter, However, the forecast Niño 3.4 value is far less than the observational value in December. The corrected forecast from the LDA method is more consistent with observations and reduces the weakening of the raw forecast in winter. For the 2010/2011 event, the raw forecast also underpredicts the Niño 3.4 index in winter, and the analog correction improves the La Niña intensity. Compared with the SFA and LA method, the LDA method also performs better in correcting model forecast (shown in the supporting information). In summary, for both mean forecast skills and ENSO events, the analog correction improves the forecasts of the ZC model.

5. Conclusions and Discussion

This works explores the application of the LDA method to model forecast corrections. The approach assumes that the forecast field can be regarded as a small disturbance superimposed on historical analogous states, and that it is possible to incorporate statistical forecasting results into numerical forecasts (Huang et al., 1993; Ren & Chou, 2007). We locate analogous states from the historical data using the LDA method. Similarities exist between a state and its analogous states, in observations, model forecasts, and model forecast errors. This ensures that unknown forecast errors can be estimated using known forecast errors of analogous states from historical data.

Here, we choose the ENSO forecast results of the ZC model for an analog-based correction experiment. Results show that the LDA method performs better than does a traditional analog method in obtaining high-quality analogs which is due to evolution dynamical information included and low-dimensional corrected object focused in the LDA method. LDA is a promising method to locate dynamic analogs. The application of analogs in model forecast error correction demonstrates the potential for improving forecast performance using the LDA method. The LDA improvements are always positive in different lead times and evaluation decades. While correlation improvements are not statistically significant at 90% of confidence

level in Figures 3a and 3c, RMSE skill and ENSO events demonstrate significant positive improvements from the LDA method. The improvement quality from the LDA method is dependent on the evaluation period and indicators. For correlation skill, the improved quality in the last decade is more obvious than that in the other decades, which is interesting for operational ENSO forecast. The improvement also depends on model. Applied to Climate Forecast System version 2, the improvements of correlation skill of Niño 4 index pass 90% of confidence level in the lead time of 2 to 9 months over the period of January 1982 to December 2018 (no shown). The LDA method has the advantages of convenient calculation, time saving, and wide application range. In the following study, the LDA method will be applied to more operational model forecasts.

Data Availability Statement

The Kaplan data are available at the website (https://www.esrl.noaa.gov/psd/data/gridded/data.kaplan_sst.html). We acknowledge the support of the Center for High Performance Computing and System Simulation, Qingdao Pilot National Laboratory for Marine Science and Technology.

Acknowledgments
This work was supported by the Fundamental Research Funds for the Central Universities (201962009) and National Natural Science Foundation of China (NSFC) Project (41530424; 41775100), and the Fundamental Research Funds for the Central Universities (202013031).

References

Bergen, R. E., & Harnack, R. P. (1982). Long-range temperature prediction using a simple analog approach. *Monthly Weather Review*, *110*(8), 1083–1099. https://doi.org/10.1175/1520-0493(1982)110<1083:LRTPUA>2.0.CO;2

Carter, G. M., Dallavalle, J. P., & Glahn, H. R. (1989). Statistical forecasts based on the National Meteorological Center's numerical weather prediction system. *Weather and Forecasting*, *4*(3), 401–412. https://doi.org/10.1175/1520-0434(1989)004<0401:sfbotn>2.0.co;2

Chen, D., Cane, M. A., Kaplan, A., Zebiak, S. E., & Huang, D. (2004). Predictability of El Niño over the past 148 years. *Nature*, *428*(6984), 733–736. https://doi.org/10.1038/nature02439

Dalcher, A., & Kalnay, E. (1987). Error growth and predictability in operational ECMWF forecasts. *Tellus A*, *39*(5), 474–491. https://doi.org/10.1111/j.1600-0870.1987.tb00322.x

Danforth, C. M., & Kalnay, E. (2008). Impact of online empirical model correction on nonlinear error growth. *Geophysical Research Letters*, *35*, L24805. https://doi.org/10.1029/2008GL036239

Delsole, T., & Hou, A. Y. (1999). Empirical correction of a dynamical model. Part I: Fundamental issues. *Monthly Weather Review*, *127*(11), 2533–2545. https://doi.org/10.1175/1520-0493(1999)127<2533:ECOADM>2.0.CO;2

DelSole, T., Zhao, M., Dirmeyer, P. A., & Kirtman, B. P. (2008). Empirical correction of a coupled land-atmosphere model. *Monthly Weather Review*, *136*(11), 4063–4076. https://doi.org/10.1175/2008MWR2344.1

Duan, W. S., Tian, B., & Xu, H. (2014). Simulations of two types of El Niño events by an optimal forcing vector approach. *Climate Dynamics*, *43*(5–6), 1677–1692. https://doi.org/10.1007/s00382-013-1993-4

Duan, W. S., & Zhao, P. (2015). Revealing the most disturbing tendency error of Zebiak–Cane model associated with El Niño predictions by nonlinear forcing singular vector approach. *Climate Dynamics*, *44*(9–10), 2351–2367. https://doi.org/10.1007/s00382-014-2369-0

Glahn, H. R., & Lowry, D. A. (1972). The use of model output statistics (MOS) in objective weather forecasting. *Journal of Applied Meteorology*, *11*(8), 1203–1211. https://doi.org/10.1175/1520-0450(1972)011<1203:tuomos>2.0.co;2

Hamill, T. M., & Whitaker, J. S. (2006). Probabilistic quantitative precipitation forecasts based on reforecast analogs: Theory and application. *Monthly Weather Review*, *134*(11), 3209–3229. https://doi.org/10.1175/MWR3237.1

Hou, Z. L., Li, J. P., Ding, R. Q., Feng, J., & Duan, W. S. (2018). The application of nonlinear local Lyapunov vectors to the Zebiak–Cane model and their performance in ensemble prediction. *Climate Dynamics*, *51*(1–2), 283–304. https://doi.org/10.1007/s00382-017-3920-6

Huang, J. P., Yu, Y., Wang, S., & Chou, J. F. (1993). An analogue-dynamical long-range numerical weather prediction system incorporating historical evolution. *Quarterly Journal of the Royal Meteorological Society*, *119*(511), 547–565. https://doi.org/10.1002/qj.49711951111

Jin, E. K., Kinter, J. L. III, Wang, B., Park, C. K., Kang, I. S., Kirtman, B. P., et al. (2008). Current status of ENSO prediction skill in coupled ocean-atmosphere models. *Climate Dynamics*, *31*(6), 647–664. https://doi.org/10.1007/s00382-008-0397-3

Kaplan, A., Cane, M. A., Kushnir, Y., Clement, A. C., Blumenthal, M. B., & Rajagopalan, B. (1998). Analyses of global sea surface temperature 1856-1991. *Journal of Geophysical Research*, *103*(C9), 18,567–18,589. https://doi.org/10.1029/97JC01736

Kirtman, B. P., & Schopf, P. S. (1998). Decadal variability in ENSO predictability and prediction. *Journal of Climate*, *11*(11), 2804–2822. https://doi.org/10.1175/1520-0442(1998)011<2804:DVIEPA>2.0.CO;2

Lguensat, R., Tandeo, P., Ailliot, P., Pulido, M., & Fablet, R. (2017). The analog data assimilation. *Monthly Weather Review*, *145*(10), 4093–4107. https://doi.org/10.1175/MWR-D-16-0441.1

Li, J. P., & Ding, R. Q. (2011). Temporal-spatial distribution of atmospheric predictability limit by local dynamical analogs. *Monthly Weather Review*, *139*(10), 3265–3283. https://doi.org/10.1175/MWR-D-10-05020.1

Li, J. P., & Ding, R. Q. (2013). Temporal-spatial distribution of the predictability limit of monthly sea surface temperature in the global oceans. *International Journal of Climatology*, *33*(8), 1936–1947. https://doi.org/10.1002/joc.3562

Li, J. P., & Ding, R. Q. (2015). Weather forecasting: Seasonal and interannual weather prediction. In *Encyclopedia of atmospheric sciences* (2nd ed., pp. 303–312). London: Elsevier. https://doi.org/10.1016/B978-0-12-382225-3.00463-1

Li, J. P., Feng, J., & Ding, R. Q. (2018). Attractor radius and global attractor radius and their application to the quantification of predictability limits. *Climate Dynamics*, *51*(5–6), 2359–2374. https://doi.org/10.1007/s00382-017-4017-y

Liu, Y., & Ren, H. L. (2017). Improving ENSO prediction in CFSv2 with an analogue-based correction method. *International Journal of Climatology*, *37*(15), 5035–5046. https://doi.org/10.1002/joc.5142

Lorenz, E. (1969). Atmospheric predictability as revealed by naturally occurring analogues. *Journal of the Atmospheric Sciences*, *26*(4), 636–646. https://doi.org/10.1175/1520-0469(1969)26<636:APARBN>2.0.CO;2

McPhaden, M. J., Zebiak, S. E., & Glantz, M. H. (2006). ENSO as an integrating concept in earth science. *Science*, *314*(5806), 1740–1745. https://doi.org/10.1126/science.1132588

Mu, M., Xu, H., & Duan, W. (2007). A kind of initial errors related to "spring predictability barrier" for El Niño events in Zebiak-Cane model. *Geophysical Research Letters*, *34*, L03709. https://doi.org/10.1029/2006GL027412

Ren, H. L., & Chou, J. F. (2007). Strategy and methodology of dynamical analogue prediction. *Science in China, Series D: Earth Sciences*, *50*(10), 1589–1599. https://doi.org/10.1007/s11430-007-0109-6

Ren, H. L., Zhang, P. Q., Li, W. J., & Chou, J. F. (2006). New method of dynamical analogue prediction based on multi-reference-state updating and its application. *Acta Physica Sinica*, *55*(8), 4388–4396. https://doi.org/10.7498/aps.55.4388

Tang, Y., Zhang, R. H., Liu, T., Duan, W., Yang, D., Zheng, F., et al. (2018). Progress in ENSO prediction and predictability study. *National Science Review*, *5*(6), 826–839. https://doi.org/10.1093/nsr/nwy105

Van den Dool, H. M. (1987). A Bias in skill in forecasts based on analogues and antilogues. *Journal of Climate and Applied Meteorology*, *26*(9), 1278–1281. https://doi.org/10.1175/1520-0450(1987)026<1278:abisif>2.0.co;2

Wang, C., Deser, C., Yu, J.-Y., DiNezio, P., & Clement, A. (2017). El Niño and southern oscillation (ENSO): A review. In *Coral reefs of the eastern tropical Pacific* (pp. 85–106). Dordrecht: Springer. https://doi.org/10.1007/978-94-017-7499-4_4

Zhang, S. Q. (2011a). A study of impacts of coupled model initial shocks and state-parameter optimization on climate predictions using a simple pycnocline prediction model. *Journal of Climate*, *24*(23), 6210–6226. https://doi.org/10.1175/JCLI-D-10-05003.1

Zhang, S. Q. (2011b). Impact of observation-optimized model parameters on decadal predictions: Simulation with a simple pycnocline prediction model. *Geophysical Research Letters*, *38*, L02702. https://doi.org/10.1029/2010GL046133

Zhang, S. Q., Harrison, M. J., Rosati, A., & Wittenberg, A. (2007). System design and evaluation of coupled ensemble data assimilation for global oceanic climate studies. *Monthly Weather Review*, *135*(10), 3541–3564. https://doi.org/10.1175/MWR3466.1

Zhang, S. Q., Liu, Z., Rosati, A., & Delworth, T. (2012). A study of enhancive parameter correction with coupled data assimilation for climate estimation and prediction using a simple coupled model. *Tellus, Series A: Dynamic Meteorology and Oceanography*, *64*(1), 10963. https://doi.org/10.3402/tellusa.v64i0.10963

Zhu, J. S., Huang, B., Marx, L., Kinter, J. L., Balmaseda, M. A., Zhang, R. H., & Hu, Z. Z. (2012). Ensemble ENSO hindcasts initialized from multiple ocean analyses. *Geophysical Research Letters*, *39*, L09602. https://doi.org/10.1029/2012GL051503

Zhu, J. S., Kumar, A., Lee, H. C., & Wang, H. (2017). Seasonal predictions using a simple ocean initialization scheme. *Climate Dynamics*, *49*(11–12), 3989–4007. https://doi.org/10.1007/s00382-017-3556-6

Zhu, J. S., Kumar, A., Wang, W., Hu, Z. Z., Huang, B., & Balmaseda, M. A. (2017). Importance of convective parameterization in ENSO predictions. *Geophysical Research Letters*, *44*, 6334–6342. https://doi.org/10.1002/2017GL073669